Assessing the Radioactivity Level of Seawater and Sand Samples from the Baltic Sea Region

Artūras Jukna (arturas.jukna@vilniustech.lt)
VILNIUS TECH
Gražina Grigaliūnaitė-Vonsevičienė
VILNIUS TECH

Article

Keywords:

Posted Date: September 14th, 2022

DOI: https://doi.org/10.21203/rs.3.rs-2021471/v1

Abstract

Current work reports on a novel method for determining radionuclide concentration and radioactivity in seawater by comparing the gamma-ray spectra of water-free samples of seawater and foreshore sand flooded by waves. By applying the proposed method, it is possible to save time and effort that are used to monitor the quality of seawater in the Baltic Sea with its characteristic sandy shores. Foreshore sand filters seawater trapping insoluble sediments together with radionuclides brought by waves. Radiation spectra of natural and artificial radionuclides in samples of seawater, foreshore sand, and sand taken on top of the dune (reference sample) in the Juodkrante area in Lithuania, were recorded by a gamma-ray spectrometer utilizing a NaI detector. The analysis of radiation spectra in the energy range of 30–1670 keV and the identification of radionuclides were performed using computer software. The richest collection and the highest concentration of radionuclides, including Na-22, Ar-41, Sc-46, Fe-59, Y-91, Zr-97, Nb-94, and Te-132, found in the foreshore sand confirm that the sand traps them from seawater carried by waves. Simultaneous analysis of both seawater and foreshore sand spectra is a way of accurate estimation of the radionuclide concentration at the time of seawater sampling and prior to that. Using a reference sample, the NaI detector, operating at room temperature, can be exploited to make a qualitative determination of the concentration and radioactivity of radionuclides in water-free samples.

Introduction

Studies of the concentration of radionuclides and their distribution profile in air, soil, and water are very important to understand the exposures of living objects to natural and anthropogenic sources of radiation and possible health problems. Radionuclides present in seawater[1] are not dangerous to humans because water molecules can block part of the alpha-, betta-, and gamma-ray energy. However, if radionuclides are present in drinking water, dry soil and/or air we breathe, they can cause serious health problems such as cancer, anemia, osteoporosis, cataracts, bone growth, and impairments of the various diseases and immune system of all living bodies[2,3]. For this reason, monitoring the concentration of radionuclides in the environment is very important for providing information in time about potential exposures that exceed the level of natural radiation by naturally abundant radioisotopes.

The Baltic Sea, with a water volume of ~ 22 thousand km^3, is one of the most polluted seas by radionuclides in the world[4,5], where pollution will only increase, given the pace of civilization development and the needs of the countries and populations living around the sea. Seawater constantly receives naturally occurring radionuclides such as H-3, C-14, U-238, Ra-236, Po-201, and K-40 from the atmosphere with rains/fogs[6] and various man-made radionuclides from the discharges of nuclear plants operating in the Baltic Sea region[4,5], as well as from the spread of radionuclides released during the Chernobyl nuclear plant accident[7]. The water of rivers and seawater from the North Sea (mainly due to water currents) slightly dilutes the seawater from the Baltic Sea; however, the amount of water exchange per year is only approximately 3.5% of the total amount of seawater from the Baltic Sea[8]. This total water inlet rate is not enough for the Baltic Sea to regenerate even in several decades. Therefore, radionuclides from the discharges of various radioactive sources can still be detected in seawater, and their concentration in seawater can be determined through the gamma-rays spectra of water samples.

Various groups proposed a number of different methods to determine the concentration of anthropogenic radionuclides in seawater using specific chemical reactions to concentrate radionuclides from seawater samples[9]. These methods are costly and comparatively slow (it takes weeks to concentrate the sediments of the solutions)[10,11]. Furthermore, due to vertical and horizontal turbulence, the composition of radionuclides in the seawater sample taken at different time moments can vary (in the range of several orders of magnitude) depending on the speed and direction of the winds, the depth of the sample taken, the water currents, and on the water temperature, causing its salinity, on the diffusion velocity[12,13].

To increase the reliability of measurement results and simplify the method for determining naturally existing and artificial radionuclides from the discharges of nuclear objects, this work proposes exploring the foreshore sand, since flooded by seawater sand can potentially trap radionuclides. Waves constantly flood the foreshore of the Baltic Sea with a mean height of 20 to 120 cm[14]. When the seawater subsides, only part of the water returns to the sea and the other is absorbed in the sandy foreshore. In the event of an intense wave, part of the foreshore sand leaves the foreshore along with a receding wave; however, the sand left on the shore works as a sieve filtering the water and trapping insoluble particles of matter in the water to which the radionuclides have adhered. For studies of seawater pollution, the sample is taken only at a fixed time selected point, and radionuclides trapped by the foreshore sand accumulate throughout the time between sampling. Therefore, when studying the concentration of radionuclides in seawater, we propose paying attention to the concentration of radionuclides in the foreshore sand. Current work reports results of analysis of gamma-ray spectra of radionuclides in seawater and foreshore sand samples taken in the Baltic Sea coastal area in the Juodkrante region in Lithuania. The main result of this work is a demonstration that the foreshore sand can trap radionuclides from seawater and that analysis of gamma-ray spectra of both samples can help determine and estimate the footprints of radionuclides present in seawater at a time when seawater samples were not taken for analysis.

Results

Collection of samples

Seawater samples (Sample 1) of the volume of approximately 0.045 m^3 for gamma-rays spectra measurements were taken in June 2021 at a water temperature of ~283 K. Each sample was collected in the Baltic Sea coastal zone in the Juodkrante area (55^o 34‘ 57.8” N 21^o 06‘ 12.9” E) 50 meters from the coast (Figure 1) at a depth of approximately 1 m in the presence of slight waves with a height of approximately 10 cm and low turbidity.

The foreshore sand (Sample 2) from the beach face (foreshore) was taken approximately 6 m away from the coast (Figure 1). This sand was constantly flooded by seawater when the waves were greater than 20 cm. The sea waves of this height and the higher amplitudes (the latter is characteristic for winter – fall periods) are typical of the Baltic Sea[14], both in the cold and in the warm season.

Sample 3 is also the sand sample, but it was collected at the top of the approximately 10 m high dune, almost 46 m from the coast. This sand was not in direct contact with seawater, but the same as in the seawater sample and the foreshore sand sample, radionuclides in Sample 3 can be collected from atmospheric precipitates, caused by rainfall (most rainfall is around 650 mm per year) and fog (most often during winter-fall periods)[15]. Therefore, Sample 3 was used in our experiments for reference purposes.

Sample technology

All tested samples (Samples 1-3) were collected at the same time on June 21, 2021. A 44.47-liter seawater sample (Sample 1) was divided into smaller portions, heated to 100 °C, and boiled for a long time (approximately 65 hours) to evaporate fresh water and extract sediments and salt from it. The water evaporation rate was 700–800 ml per hour. At the end of the water evaporation process, the water-free sample crystallized into large crystals of salt, which were mechanically crushed into small grains with an average diameter of (7.3 ± 4.2) ´ 10^{-4} m. The residual size of the salt grains was measured and calculated using data obtained from the images of the optical microscope and assuming that all grains observable through the microscope in an area of 225 mm^2 of an optical window have an almost round shape (Figure 2). The sample preparation procedure ended with sample annealing at a temperature of 550 K for 3 hours in air at atmospheric pressure with a subsequent slow cooling (2–3 hours) to a temperature of 320 K. Then, at temperature 320 K, the water-free sample with a mass m = 0.3213 kg was immediately poured into a water-vapor-resistive container of the gamma-ray spectrometer and was ready for measurements.

The optimal annealing temperature and annealing time were estimated using references[12,13,16], and the residual water content in the water-free seawater sample was determined by weighting it before and after the annealing procedure. The percentage weight difference was calculated using the following relation: $W_s = 100\ \% \cdot (m_0 - m)/m$. Here, W_s is the relative weight, m_0 and m are the initial (*i.e.* before the procedure of annealing the sample at temperature 550 K for 3 hours) and the final (after annealing) masses of the sample, respectively. Taking into account the experimentally measured value m, the salinity of seawater was estimated at 7.23 % or 7.23 grams of dissolved salts in each liter of seawater.

The same sample drying procedure was applied for Samples 2 and 3. In the same way, they were annealed at 550 K for 3 hours in the air, slowly cooled, and, while at a temperature of 320 K, immediately poured into a plastic container so that the samples were protected against water vapor and kept dry during the entire experiment. The mean diameter of the sand grains was $(5.9 \pm 2.2) \cdot 10^{-4}$ m and $(2.4 \pm 1.1) \cdot 10^{-4}$ m in Samples 2 and 3, respectively. The average size of the particles was estimated using the optical microscope images, assuming that the sand grains, which are observed in a 225 mm^2 optical window area, are almost round. In fact, most of the sand grains in Sample 2 appear with polished edges (Figure 2), but in the sand sample taken on top of the sand dune, the grains have more unpolished, *i.e.* sharp edges. This result is in line with ref. 17.

The gamma-ray spectra measurements setup

As prepared samples were measured using a gamma-ray spectrometer, which utilizes an integrated preamplifier and a sodium iodide (NaI) detector operating at room temperature. NaI crystal with the dimensions of $76 \cdot 76$ mm^2 capable of detecting radiation energy ranging between 30.00 and 1670.85 keV with resolution of 3.205 keV and sensitivity (Cs-137) 32 000 cps/mrem/hr ± 3.5 percent. The energy (E) calibration was performed using the reference spectrum of radionuclides. The same spectrum was also used for the calculations of the gamma-ray energy vs. channel (Ch) number dependence of the spectrometer using equation $E = 10.23 + 0.4567 \cdot Ch$ as well as full-width-at-half-maximum ($FWHM = 0.9871 + 0.03463$ of energy peaks and curves of tailing of peaks (Tp) vs. energy dependence $Tp = 1.127 + E \cdot 2.053 \cdot 10^{-4}$. The energy efficiency (Eff) calibration performed using a certificate file and a polynomial fit better than 4.9 % of experimental data with calculations. It was achieved by fitting the experimental values obtained for the low energy interval (30.00–165.85 keV) using the polynomic $ln(Eff) = -6.73 + 12.80 \cdot ln(E) - 1.296 \cdot ln(E^2)$ and in the case of higher energies (166.85–1670.85 keV) using the polynomic $ln(Eff) = -134.2 + 83.98 \cdot ln(E) - 20.1 \cdot ln(E^2) + 2.105 \cdot ln(E^3)$.

For better resolution, each measurement of the gamma-ray spectrum lasted 72 hours using a measurement scheme shown in Figure 3. Since the radiation source might be assumed to be a point source, it can emit gamma-rays with the same probability at a space angle 4p. However, the detector records only the radiation that is incident onto the NaI crystal at a space angle of 1.425p. This fact was taken into account when calculating the radioactivity of the samples. Furthermore, to better compare the spectra of Samples 1–3, each time the same volumetric amount of testing material was poured into a measuring container (Figure 3) to form a minimum of 2.5 cm thick layer of material around the cylindrical corpus with a surface area of 852 cm^2 of the detector (shown in red). Because the volume of samples was taken approximately the same and all other conditions (i.e. time of spectrum measurements, ambient temperature, and humidity) during the experiment did not change, it was possible to compare the recorded spectra of different samples and determine the radionuclide composition and radioactivity in a broad range of tested energies.

Results And Discussion

A gamma-ray spectrum of Sample 1 in the 30.00-1678.85 keV range of radiation energies is shown in Figure 4. The spectrum obtained contains characteristic lines for natural radionuclides, for example, Na-22 and Na-24 produced by cosmic radiation [18] and K-40 [19]. The rest of radionuclides, such as those of Eu-152, Co-57, Ce-144, Xe-138, Xe-131M, Ce-139, Ba-139, Kr-88, Xe-125, Fe-59, Te-132, Xe-133M, Nb-95M, Sr-92, Xe-135, Cr-51, Bi-211, Zr-97, Y-94, I-126, Sn-113, Kr-87, Pb-211, Zn-69M, Y-92, Nb-96, I-124, Sb-124, Bi-214, Ru-106, Nb-95, Rb-88, Y-88, Zr-89, Zn-65, Co-60, Cu-64 are of

anthropogenic origin[18]. These results confirm that the NaI detector can be used successfully to quantitatively determine radionuclides and their concentration in dry seawater sediments and salt from the Baltic Sea containing natural and anthropogenic radionuclides[20].

The observed peaks of radiated energy in the spectrum (Figure 4) are relatively broad (10–30 keV). Most of these peaks are made up of closely located and overlapping multiple peaks. Therefore, their amplitude and FWHM can only be resolved using computer software developed for the gamma-ray spectra analysis and radionuclides' identification. The shape of the spectra of Samples 2 and 3 (not shown here) was very similar but indicated different radionuclide compositions and/or a different level of their activity.

The analysis of data given below in Table 1 indicates that Sample 2 (i.e. foreshore sand frequently flooded by waves) is the richest of radionuclides. This result is explained by assuming that the water brought by the sea wave partially absorbed into the sand is filtered and the substances/sediments insoluble in seawater with radionuclides stick to the sand grains.

Table 1. Radionuclides detected in water-free Samples 1–3. The light grey rows in the table represent the radionuclides identified in the spectra of all samples. The radionuclides that emit several spectral lines (the numeral of additional spectral lines is presented by a numerical value in parentheses) are bolded. The bold white symbols in dark grey cells represent the radionuclide detected only in the foreshore sand.

Radionuclides in Sample 1 (Seawater)	Id confidence	Radionuclides in Sample 2 (Foreshore sand)	Id confidence	Radionuclides in Sample 3 (Sand on a top of dune)	Id confidence	Energy, keV	Half-life
		Na-22	0.815			1274.54	2.6019y
Na-24	0.999	Na-24	0.929	Na-24	0.921	1368.53	14.96h
		Ar-41	0.923			1293.64	109.61m
				K-40	0.865	1460.81	1.28×10^{9}y
		Sc-46$_{(1)}$	0.922			889.25	83.79d
Cr-51	0.952	Cr-51	1.000	Cr-51	1.000	320.08	27.7025d
		Fe-59$_{(3)}$	0.943			142.65	44.495d
Co-57$_{(1)}$	0.831	Co-57	0.823			122.06	271.74d
Co-60$_{(1)}$	0.844					1173.22	5.2713y
Cu-64	0.959	Cu-64	0.967			1345.90	12.700h
Zn-65	0.979	Zn-65	0.890	Zn-65	0.919	1115.52	243.66d
Zn-69M	1.000					438.63	13.76h
		Kr-85M$_{(1)}$	0.996	Kr-85M	0.996	151.18	4.480h
Kr-87$_{(1)}$	0.749	**Kr-87**$_{(1)}$	0.764	Kr-87	0.802	402.58	76.3m
Rb-88	0.931	Rb-88	1.000	Rb-88	0.934	898.02	17.773m
Sr-92$_{(4)}$	0.964	**Sr-92**$_{(3)}$	0.636	Sr-92	0.861	241.52	2.66h
Y-88	0.916	Y-88	0.999	Y-88	0.920	898.02	106.616d
		Y-91	0.940			557.57	58.51d
Y-94$_{(3)}$	0.839	**Y-94**$_{(3)}$	0.843	Y-94	0.786	381.60	18.7m
Zr-89	0.910	Zr-89	0.909	Zr-89	0.996	909.10	78.41(12)h
Zr-97$_{(4)}$	0.884					355.39	
		Zr-97	0.786			1362.66	16.744h
		Nb-94$_{(1)}$	0.959			702.63	2.03×10^{4}y
Nb-95	0.972			Nb-95	0.962	765.79	23.35h
Nb-95M	1.000	**Nb-95M**$_{(3)}$	0.988	Nb-95M	0.994	235.69	3.61d
		Mo-99$_{(3)}$	0.918	Mo-99	0.942	140.51	2.7489d
		Tc-99M	0.985	Tc-99M	0.984	140.51	6.0067h
Ru-106	0.800	Ru-106	0.908	Ru-106	0.775	621.84	373.59d
Sn-113	0.957	Sn-113	0.947	Sn-113	0.947	391.69	115.09d

		Sb-122$_{(1)}$	0.964	Sb-122	0.826	563.93	2.7238d
		Te-132$_{(1)}$	0.966			116.30	3.204d
Te-132	0.911					228.16	
I-126	0.992	I-126	0.997	I-126	0.994	388.63	12.93d
I-124$_{(1)}$	0.957	**I-124$_{(1)}$**	0.926	I-124	0.815	602.71	4.1760d
Xe-125$_{(1)}$	0.985	**Xe-125$_{(1)}$**	0.989	Xe-125	0.993	188.43	16.9h
Xe-131M	1.000	Xe-131M	0.993	Xe-131M	0.995	163.93	11.934d
Xe-133M	0.999	Xe-133M	0.993	Xe-133M	0.997	233.22	2.19d
Ba-139	1.000	Ba-139	0.990	Ba-139	0.992	165.85	83.06m
Ce-139	1.000	Ce-139	0.990	Ce-139	0.992	165.85	137.641d
				Ce-141	0.993	145.44	32.508d
Bi-214$_{(4)}$	0.803			Bi-214	0.572	609.31	19.9m
				Ra-226	0.999	186.21	1.602×10^{3}y
				Th-232	0.997	59.00	1.4×10^{10}y
		Am-241	0.996	Am-241	0.996	59.54	432.2y

The radionuclides shown in Table 1 were identified with identification confidence (further id confidence) greater than 0.8 using the spectrometer radionuclide library. Factors such as data acquisition, calibration drift, temperature change, and background radiation[21] can cause incorrect identifications, and therefore radionuclides with id confidence less than 0.8, were skipped. For better clarity of the results, the radionuclides found in all three samples are colored grey in Table 1 and the radionuclides that are characteristic only for the foreshore sand (Sample 2) are shown by white symbols in grey cells in this table. Radionuclides that exhibit more than one spectral line are bolded with a subscript in parentheses representing a number of additional spectral lines detected by the computer program. According to our data, the water-free seawater spectrum (Sample 1) contains a 19 % lower number of identified radionuclides and the dune sand is characterized by an almost 49 % lower number of radionuclides with id confidence greater than 0.8. It should be mentioned that natural radionuclides (*e.g.* K-40, Cd-109, I-125, Bi-207, Th-228, U-238, Pu-239) were not identified in the spectra, which is explained by possibly too low radioactivity of natural radionuclides compared to anthropogenic sources of gamma-radiation, the too high amplitude of a background signal, and possible evaporation of a part of radionuclides together with water vapor during the drying process of the samples.

Due to naturally occurring water streams and waves, any seawater sample taken in the coastal area at a particular moment holds only a random concentration of radionuclides. It cannot contain information on what the concentration of radionuclides was yesterday or a month ago. Therefore, simultaneous analysis of spectra of Samples 1–3 is one of the most important measures to collect information on the presence of e.g. undeclared nuclear activities in the Baltic Sea region. On the other hand, small amounts of radionuclides in air, water, and soil, and the radionuclides themselves and their concentration in the environment provide information on the processes that can possibly cause radionuclides to arise[5,7]. Among all detected radionuclides, radionuclides of anthropogenic origin make up the largest part (Table 1). The results presented above show that some of the anthropogenic radionuclides such as Zn-65, Kr-87, Kr-88, Rb-88, Sr-92, Y-88, Y-94, Nb-95M, I-124, I-126, Xe-125, Xe-131M, Xe-133M, Ba-139 and Ce-139 are present in all samples tested (rows marked grey in Table 1) and could be associated with atmospheric pollutants originated from discharges of radioactive pollution from

nuclear objects located near the Baltic Sea. Later, winds and rains brought these pollutants to the Juodkrante area. Later, winds and rains brought these pollutants to the Juodkrante area.

The assumption that the foreshore sand traps some of the radionuclides from seawater brought by waves confirms the results shown by a diagram of radioactivity versus radionuclides (Figure 5), which represents the radioactivity of radionuclides identified with high values of id confidence in all three types of samples. The highest values of radioactivity were determined for the foreshore sand with the highest magnitude of radioactivity ranging between 17 and 20 Bq kg^{-1} attributed to radionuclides Kr-88, Xe-131M, Ba-139, and Ce-139. The lowest radioactivity, but with the same high id confidence, was determined for Na-24 decaying with a half-life of 15 hours to the daughter isotope Mg-24 (i.e. cosmogenic nuclide) and Zn-65 decaying to Cu-65 with a half-life of 244 days.

The results discussed in the current work are based on investigations of surface sand (at depths of 10 to 20 cm). The concentration of radionuclides in the sand granules/crystals depends on many factors[22]. These are the rate of diffusion of radionuclide (or its carrier) through the absorption of sand, the radionuclide (or its carrier) by the sand, the porosity of the sand, the character of its pore constriction when water penetrates through the sand, tortuosity of the intergranular channels (water drains), and on the dimensions and morphology of radionuclide (or its carrier). Estimating the transport of radionuclides through the foreshore sand with more accuracy and their trapping by sand requires more experimental data, which can help to prove the estimation of the presence of radionuclides in seawater in the Baltic Sea (or another large body of salted or freshwater) at a time interval between water samples taken for analysis.

The detected radionuclides and their id confidence values are related to radionuclide library configuration, which is used in computer software for radionuclide detection and identification. The software detected a 1460 keV peak of K-40, which decays predominantly by b-emission to Ca-40, but not in the three samples. The library used in the current experiments identified K-40 in Sample 3 (Table 1) but did not find it in other samples. Better sensitivity can be achieved using the CdTe and / or HPGe detectors. As shown in the work[20], the NaI detector has the highest efficiency and the lowest minimum detectable activity compared to the HPGe and/or CdTe detectors. Therefore, measurement results using CdTe or HPGe detectors may result in better resolution and identification of radionuclides in seawater and foreshore sand. Furthermore, the concentration of radionuclide K-40 can decrease below a resolution limit of the spectrometer during the process of preparing water-free samples, *i.e.* some part of radionuclides can evaporate together with water and other light and volatile components (radionuclide carriers) present in samples of seawater and sand.

It should be mentioned that underground nuclear weapons explosions[23] and nuclear reactor operations[24] release gaseous species Xe-125, Xe-131M and Xe-133 gaseous species into the atmosphere. The presence of these isotopes indicates that the necessity for human activities related to nuclear power is constantly increasing[24]. Because of their inert nature and relatively short half-life, Xe isotopes do not present an appreciable long-term health hazard but can be used as a tracer for the identification of radionuclide distribution in seawater. The highest concentration of isotopes Xe-125, Xe-131M, and Xe-133 has been found in the foreshore sand (Sample 2) and the lowest in the unflooded seawater sand taken at the top of a dune (Sample 3). This detected difference between Sample 2 and Sample 3 in radionuclide concentration (Figure 5) shows that the foreshore sand can trap radionuclides from the seawater and, for more reliable monitoring of seawater quality, the gamma-spectrum of seawater has to be investigated together with the spectrum of the foreshore sand.

Conclusions

The current work presents a novel method for detecting radionuclides and their concentration in seawater. The Baltic Sea near Juodkrante in Lithuania is mainly polluted by radioactive anthropogenic radioisotopes of krypton, strontium, yttrium, niobium, iodine, xenon, barium, and cerium with the highest concentration found in the foreshore sand frequently flooded by waves. Radionuclides obtained only in the foreshore sand such as Na-22, Ar-41, Sc-46, Fe-59, Y-91, Zr-97, Nb-94, and Te-132 were found in neither in the seawater sample nor in the sand sample, taken at the top of the dune. Current experimental

results show that the concentration and variety obtained in the seawater sample vary over time, possibly depending on wind direction, water streams, waves' height, water temperature, *etc*. However, even if the seawater sample is taken only once per year, the pollution by radionuclides in seawater can be still monitored by using an analysis of the gamma-spectrum of seawater together with the spectrum of the foreshore sand, since the last can trap radionuclides from seawater during the period between seawater sampling. This method simplifies the monitoring of seawater quality.

Current results also let concluding that a NaI-based gamma-ray detector, operating at room temperature, can be applied for the quantitative determination of radionuclide concentrations in water-free samples of seawater and foreshore sand if their gamma-spectra are recorded at least for 72 hours and the samples are well protected against water vapor during the entire experiment. However, the CdTe and/or HPGe detectors have to be used for higher precision of identification of radionuclides, more precise measurements of the area of energy peaks, and the full-width-at-half-maximum for each line in the energy spectrum. As shown in the references in the current work, the NaI detector has the highest efficiency but the lowest minimum detectable activity, compared to those of the HPGe and/or CdTe detectors, which better address partially overlapping energy peaks of radionuclide radiation. However, the proposed method for radionuclide and their concentration detection utilizing the NaI-based gamma-ray detector is recommended by authors for regular seawater pollution monitoring, especially in the case of the Baltic Sea, as the foreshore sand of the Baltic Sea constantly collects radionuclides during the period between seawater sampling.

Declarations

Author contributions statement

A.J. conducted the experiments, analyzed the results, prepared figures 1-4, and wrote the main manuscript text and G.G.V. analyzed the results and prepared figure 5 and table 1. All authors reviewed the manuscript.

Additional information

The authors declare that the research was conducted in the absence of commercial or financial relationships that could be construed as a potential conflict of interest.

Data availability

All data generated or analyzed during this study are included in this published article.

References

1. Baskaran, M., Hong, G. -H., Santschi, P. H. Radionuclide analysis in seawater. *Practical guidelines for the analysis of seawater* (Ed. by oLIVER Wurl). CRC Press Taylor & Francis Group. Chapter 13, 260–295 and references therein. https://doi.org/10.1201/9781420073072 (2009).
2. Canu, I. G., Laurent, O., Pires, N., Laurier, D., Dublineau, I. Health effects of naturally radioactive water ingestion: the need for enhanced studies. *Environ. Health Perspect.* 119 (12), 1676–1680. https://doi.org/10.1289/ehp.1003224 (2011).
3. Priasetyono, Y., Makmur, M., Suseno, H., Prihatiningsih, W. R., Yahya, M. Y., Putra, D. I. P. The natural radionuclide activity and the risk of potential radiation in health effect: a study on beach sand in Madura, Bali, and Lombok. *J. Kesehatan Lingkungan* 13 (3), 142–150. http://dx.doi.org/10.20473/jkl.v13i3.2021.142-150 (2021).
4. Garnaga-Budre, G. Integrated assessment of pollution in the Baltic Sea. *Ekologija* 58 (3), 331–355. https://doi.org/10.6001/ekologija.v58i3.2531 (2012).
5. Qiao, J., Zhang, H., Steier, P., Hain, K., Hou, X., Vartti, V. -P., Henderson, G. M., Eriksson, M., Aldahan, A., Possnert, G., Golser, R. An unknown source of reactor radionuclides in the Baltic Sea revealed by multi-isotope fingerprints. *Nat. Commun.* 12, 823 (1–10). https://doi.org/10.1038/s41467-021-21059-w (2021).

6. Vasconcelos, D. C., Pereira, C., Oliveira, A. H., Santos, T. O., Rocha, Z., Menezes, M. A. B. C. Determination of natural radioactivity in beach sand in the extreme south of Bahia, Brazil, using gamma spectrometry. *Rad. Prot. Environ.* 34(3), 178–184. https://doi.org/10.4103/0972-0464.101714 (2011).
7. Sulaiman, S. N. A., Mohamed, F., Rahim A. N. A. Radioactive release during nuclear accidents in Chernobyl and Fukushima. *IOP Conf. Series: Materials Science and Engineering* 298, 012011. https://doi.org/10.1088/1757-899x/298/1/012011 (2018).
8. Håkanson, L., Bryhn, A. Water Exchange and Water Transport in the Baltic Sea. *Eutrophication in the Baltic Sea. Environmental Science and Engineering*. Springer, Berlin, Heidelberg. Ch.3, 69–89. https://doi.org/10.1007/978-3-540-70909-1_3 (2008).
9. Aoyama, M., Hirose, K. Radiometric determination of anthropogenic radionuclides in seawater. Analysis of Environmental Radionuclides. *J. Environ. Radioact.* 11, 137–162. https://doi.org/10.1016/S1569-4860(07)11004-4 (2008).
10. Shiozaki, M., Seto, Y., Higano, R. Simplified Analytical Method of Strontium 90 in Sea Water. *J. Oceanograph. Soc. of Japan* 20 (1), 7–13. https://doi.org/10.5928/kaiyou1942.20.7 (1964).
11. Borcherding, J., Nies, H. An improved method for the determination of ^{90}Sr in large samples of seawater. *J. Radioanal. Nucl. Chem.* 98 (1), 127–131. https://doi.org/10.1007/BF02060440 (1986).
12. Albinsson, Y., Andersson, K., Börjesson, S., Allard, B. Diffusion of radionuclides in concrete and concrete-bentonite systems. *J. Contam. Hydrol.* 21, 189–200. https://doi.org/10.1016/0169-7722(95)00046-1 (1996).
13. Iaffaldano, G., Caputo, M., Martino, S. Experimental and theoretical memory diffusion of water in sand. *Hydrol Earth Syst Sci.* 10, 93–100. https://doi.org/10.5194/hess-10-93-2006 (2006).
14. Kelpšaitė, L., Herrmann, H., Soomere, T. Wave regime differences along the eastern coast of the Baltic Proper. *Oceanogr.* 57 (4), 225–231. https://doi.org/10.3176/proc.2008.4.04 (2008).
15. Meier, H. E. M., Kniebusch, M., Dieterich, Ch., Gröger, M., Zorita, E., Elmgren, R., Myrberg, K., Ahola, M. P., Bartosova, A., Bonsdorff, E., Börgel1, F., Capell, R., Carlén, I., Carlund, T., Carstensen, J., Christensen, O. B., Dierschke, V., Frauen, C., Frederiksen, M., Gaget, E., Galatius, A., Haapala, J. J., Halkka, A., Hugelius, G., Hünicke, B., Jaagus, J., Jüssi, M., Käyhkö, J., Kirchner, N., Kjellström, E., Kulinski, K., Lehmann, A., Lindström, G., May, W., Miller, P. A., Mohrholz, V., Müller-Karulis, B., Pavón-Jordán, D., Quante, M., Reckermann, M., Rutgersson, A., Savchuk, O. P., Stendel, M., Tuomi, L., Viitasalo, M., Weisse, R., Zhang, W. Climate change in the Baltic Sea region: a summary. *Earth Syst. Dyn.* 13, 457–593. https://doi.org/10.5194/esd-13-457-2022 (2022).
16. Ding, Y, Hassanali, A. A., Parrinello, M. Anomalous water diffusion in salt solutions. *PNAS* 111 (9), 3310–3319. https://doi.org/10.1073/pnas.1400675111 (2014).
17. Skuodis, S. DEM Simulation Based on Experimental Testing (Ch. 11) in *Modeling and Simulation in Engineering Sciences* (*ed. by* Akbar, N. Sh. and Beg, O. A.), 245–264. https://doi.org/10.5772/63889 (2016).
18. Omar, M., Laili, Z., Wood, A. K., Karim, J. A., Masood, Z., Zakaria, M. F., Saad, M. F. A systematic approach in the gamma spectrometric determination of radionuclides in coolant of Puspati Triga reactor. *Jurnal Sains Nuklear Malaysia* 23(2), 1–11. https://inis.iaea.org/search/search.aspx?orig_q=RN:43055409 (2011).
19. Alaamer, A. S. Measurement of Natural Radioactivity in Sand Samples Collected from Ad-Dahna Desert in Saudi Arabia. *World J. Nucl. Sci. Technol.* 2, 187–191. https://doi.org/10.4236/wjnst.2012.24029 (2012).
20. Perez-Andujara, A., Pibidab, A. Performance of CdTe, HPGe and NaI(Tl) detectors for radioactivity measurements. *Appl. Radiat. Isot.* 60, 41–47. https://doi.org/10.1016/j.apradiso.2003.10.006 (2014).
21. Pibida L., Untyerweger M., Karam L. R. Evaluation of handled radionuclide identifiers. *J. Res. Natl. Inst. Stand. Technol.* 109 (4), 451–456. https://doi.org/10.6028/jres.109.032 (2004).
22. Uosif, M.A.M., Alrowaili, Z.A., Elsaman, R., Mostafa, A.M.A. Soil–soybean transfer factor of natural radionuclides in different soil textures and the assessment of committed effective dose. *Radiat. Prot. Dosimetry* 188(4), 529–535.

https://doi.org/10.1093/rpd/ncaa005 (2020).

23. Peräjärvi, K., Eronen, T., Gorelov, D., Hakala, J., Jokinen, A., Kettunen, H., Kolhinen, V., Laitinen, M., Moore, I. D., Penttilä, H., Rissanen, J., Saastamoinen, A., Toivonen, H., Turunen, J, Äystö, J. Production of pure ^{133m}Xe for CTBTO. *Hyperfine Interact.* 223, 239–243. https://doi.org/10.1007/s10751-012-0626-3 (2014).
24. Cohen, N., Lo Sasso, T., Lei, W. ^{133}Xe and ^{135}Xe interference with in vivo low-energy measurement systems. *International Nuclear Information System (INIS)* 38 (3), 414–416. https://worldwidescience.org/topicpages/x/xe-131m+xe-133+xe-133m.html (1980).

Figures

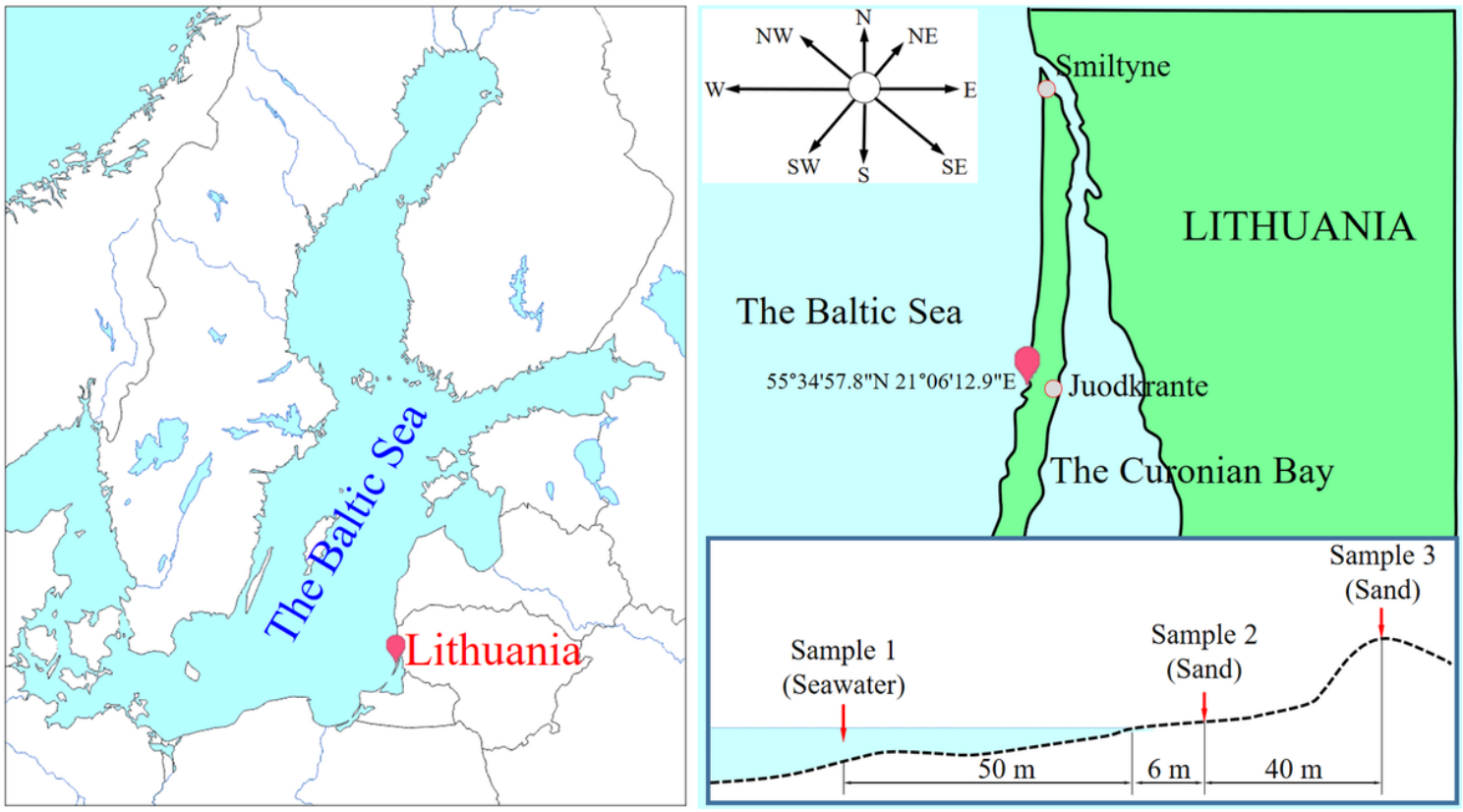

Figure 1

The global coordinates (red points on the map) for sampling seawater and sand are 55o 34' 57.8" N 21o 06' 12.9" E. The sampling (bottom corner on the right) demonstrates that Sample 1 is seawater taken at a distance of 50 m from the shoreline. Sample 2 is foreshore sand (*i.e.* sand flooded by sea waves) taken at a distance of 6 m from the water line at waves in height of approximately 10 cm. Sample 3 is sand from the top of a 10-m-high dune located at 46 m from a shoreline and not flooded by sea waves. The wind rose shows the prevailing wind direction in the Juodkrante area, Lithuania.

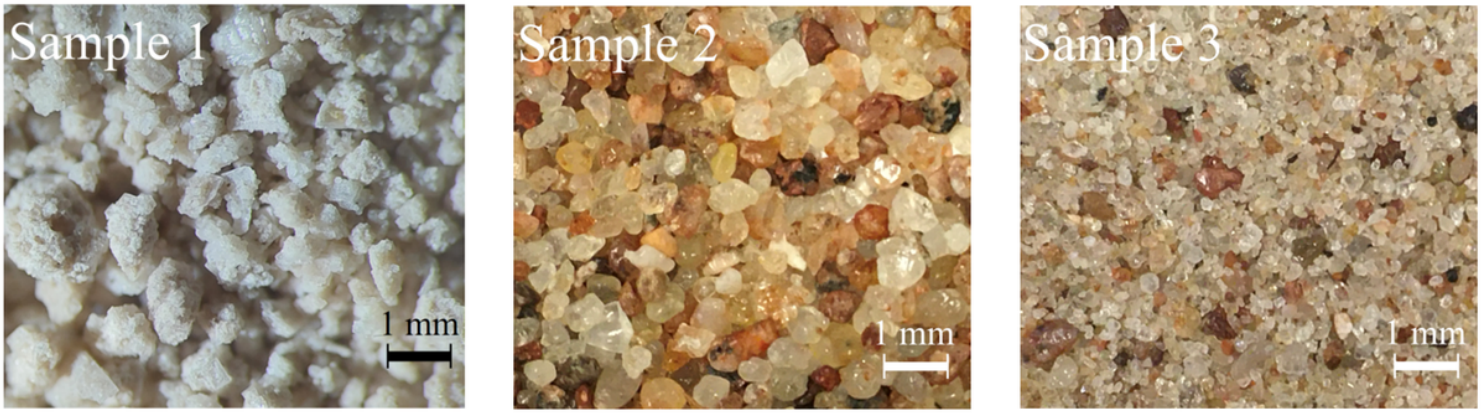

Figure 2

Optical images of three samples tested after calcination at a temperature of 550 K for 3 hours at atmospheric pressure in the air: seawater (Sample 1), foreshore sand frequently flooded by stormy sea waves (Sample 2), and sand taken at the top of the sand dune, i.e. not flooded by sea waves (Sample 3).

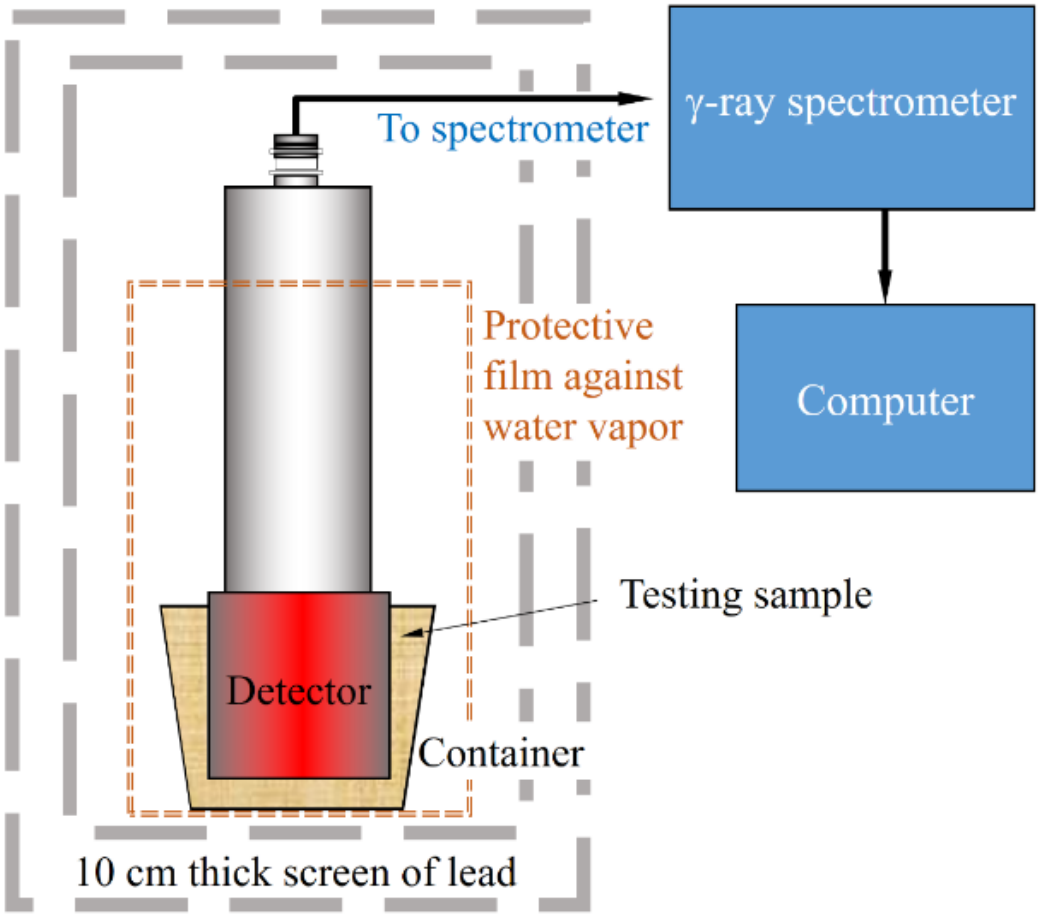

Figure 3

A water-free sample at a temperature of 320 K was poured into a container so that at least a 2.5 cm layer of testing material surrounds a NaI detector. The sample and detector are wrapped with a film, which blocks the diffusion of environmental water vapor, and moved into a screening box with 10 cm thick walls of lead, which absorbs the environmental gamma radiation.

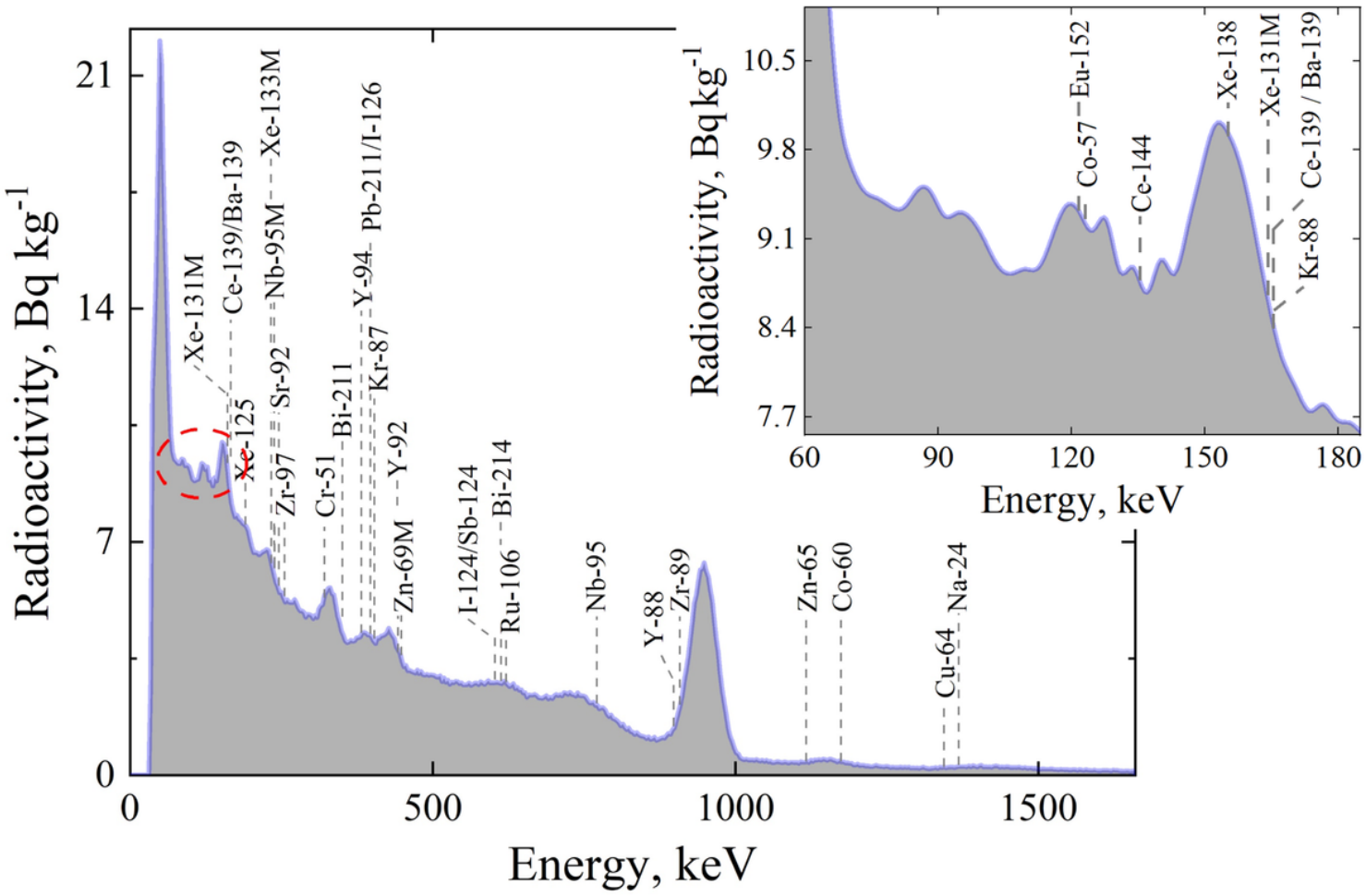

Figure 4

Radioactivity of a water-free seawater sample (Sample 1) with mass m = 0.3213 kg prepared from 44.47 liters of seawater taken in the Baltic Sea in the Juodkrante area in Lithuania in June 2021. The inset represents radioactivity at low-energy radiation by the same sample in an expanded scale in the interval of energies marked by a dashed (red) line.

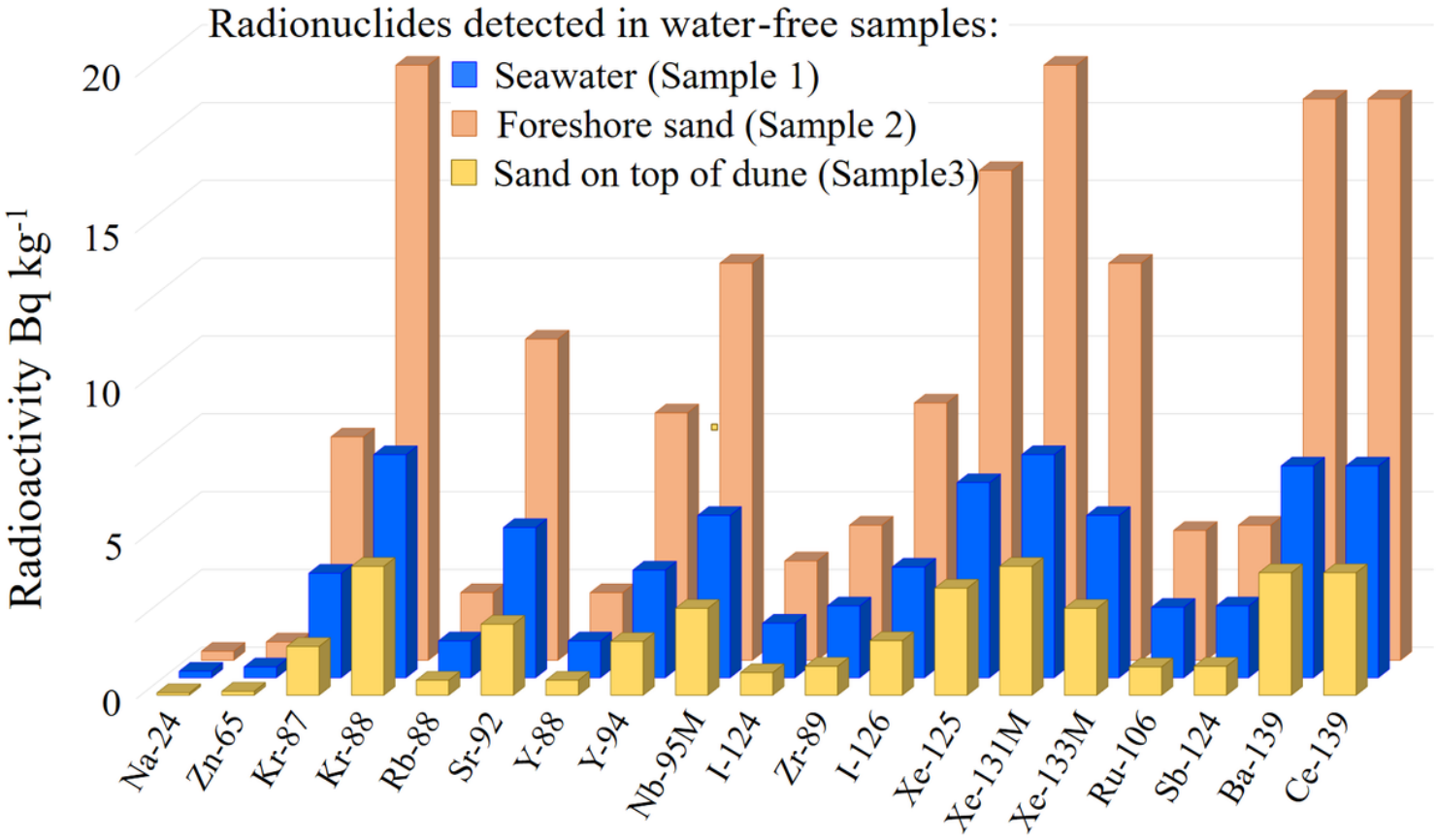

Figure 5

Radionuclides detected in water-free samples: seawater (Sample 1), sand on the foreshore (Sample 2), and sand on top of the dune (Sample 3). The highest concentration of radionuclides in the foreshore sand is explained by the trapping of radionuclides brought by the stormy sea waves.